ASSESSING HELICOPTER RECOVERY TO AN OFFSHORE PLATFORM USING PILOTED FLIGHT SIMULATION AND TIME-ACCURATE AIRWAKES

Neale A. Watson[1], *nawatson@liverpool.ac.uk*, Ieuan Owen[1], *i.owen@liverpool.ac.uk*,
Mark Prior[2], *mark@mpriorconsulting.com* & Mark D. White[1], *mdw@liverpool.ac.uk*

[1]School of Engineering, University of Liverpool, United Kingdom
[2]M Prior Consulting Ltd, United Kingdom

Abstract

This paper describes an investigation in which piloted flight simulation has been used to study the effect of turbulent air flow on helicopter recovery to an offshore platform. A helicopter flight simulation environment has been developed in which the unsteady air flow over a full-scale offshore platform has been modelled using time-accurate Computational Fluid Dynamics. Real-time piloted helideck landings have been conducted in a six-degree-of-freedom motion flight simulator where a flight dynamics model representative of a Sikorsky SH-60B Seahawk helicopter was integrated with 30 seconds of unsteady computed air flow. A test pilot was instructed to perform landings to the helideck of the platform for wind speeds of 20 to 50 kt. Ratings of pilot workload and turbulence were obtained during the trial which, along with the recorded pilot control inputs and helicopter states, were used to analyse the effect of the platform's airwake on the helicopter and on pilot workload. The results show that as the freestream wind speed increased, the turbulence intensity and pilot workload also increased. The workload ratings, along with the corresponding pilot control activity and helicopter positional accuracy, are discussed in relation to the airwake to which the helicopter was subjected. The paper demonstrates how flight simulation with time-accurate airwakes could be used to support helicopter operations to offshore platforms.

1 Introduction

Helicopters are routinely employed on offshore platforms to provide crew and freight transportation, equipment inspection, and, in emergencies, evacuation and search and rescue missions. While rotorcraft are versatile and offer a wide range of capabilities for offshore services, the environment in which they operate can be challenging [1]. If flying conditions deteriorate to a level at which the helicopter is unable to conduct missions, operational capability of the offshore platform may be reduced, leading to significant commercial penalties. Pilots may have to contend with adverse weather conditions, exhaust gas from the platform's gas turbines and flarestacks, low visibility and, once in close proximity to the platform, the unsteady air flow generated by the wind moving over and around the platform's structure; this turbulent air flow is known as the *'airwake'*. Figure 1 shows the typical position of a platform helideck in the vicinity of several large top deck structures [2].

In a survey of pilots [3], the principal safety hazard and source of the highest pilot workload during helicopter operations to offshore platforms was attributed to airwake turbulence. To ensure safe operation, a set of restrictions are defined for each offshore platform, known as the Helicopter Limitations List, HLL, by an agency responsible for the certification of the helideck [4]. Entries to the HLL are specific to particular combinations of wind speed and direction, and either restrict helicopter weight, or prevent flying altogether. To reduce the possible operational restrictions placed on an offshore platform by the HLL, due to environmental effects such as the unsteady airwake, guidelines are available to platform designers [5]. Furthermore, in preparation for helicopter operations to new offshore helidecks, or platforms with recently modified topside structures, the Civil Aviation Authority, CAA, and Norsk Sokkels Konkurranseposisjon, NORSOK, both require that the helideck must be subject to appropriate wind tunnel testing or Computational Fluid Dynamics, CFD, analysis to establish the wind environment in which helicopters will be expected to operate [1,6]. While there is a requirement to model the air flow over the flight

deck, the type of CFD turbulence modelling is not stipulated and is therefore often limited to low-cost time-averaged analyses [7–11]. Winds passing over the complex and non-aerodynamic geometry of offshore platforms typically generate unsteady airwakes dominated by both quasi-periodic, large-scale structures and chaotic small-scale turbulent features which are not well captured using time-averaged CFD analysis, leading to more emphasis and reliance on wind tunnel testing [12–14]. Steady CFD-generated airflows have been integrated with piloted flight simulation in an attempt to analyse the effect of the airwake on pilot workload; however, it was necessary to add synthetic turbulence to the computed mean airwake velocities to simulate the unsteadiness [9]. Airwake data measured in a wind tunnel has also been integrated with piloted flight simulation but, due to restrictions on computational memory, only the vertical velocity component of the airwake was processed by the helicopter flight dynamics model [15].

Figure 1: Offshore platform helicopter operations [2].

While the number of studies into the effect of turbulent airwakes on helicopters operating to offshore platforms is limited, there have been many studies into helicopters operating to naval ships, such as frigates, destroyers and aircraft carriers [16–18]. These studies have shown that unsteady computation of the airwake is essential for high-fidelity flight simulation [19]. In this paper, time accurate CFD method Delayed Detached Eddy Simulation, DDES, was used to generate the airwake of a typical semi-submersible offshore platform at one wind heading. The effect of the airwake on pilot workload during helicopter recovery to the platform's helideck was analysed by integrating the three-component unsteady velocities of the airwake with a helicopter flight dynamics model within a simulated environment in which a piloted flight trial was conducted at different wind speeds. This paper describes the development of the simulation environment and presents some of the results from the piloted flight trials.

2 The Offshore Platform

A three-dimensional model of the offshore platform used in this study was created to represent a typical semi-submersible. Shown in Figure 2, the CAD model is characterised by a large clad drilling derrick located at the centre of the platform, which is supported by six legs. (The two submerged supporting pontoons were not included as they are beneath the water surface). The helideck is positioned off the corner of the platform and there are a number of characteristic features on the platform such as cranes, gas turbine exhaust stacks and structural modules. The platform is 83 m wide, 117 m long with the top of the clad derrick reaching a height, H, of 100 m above sea level. The height of the helideck above the sea surface is 36 m.

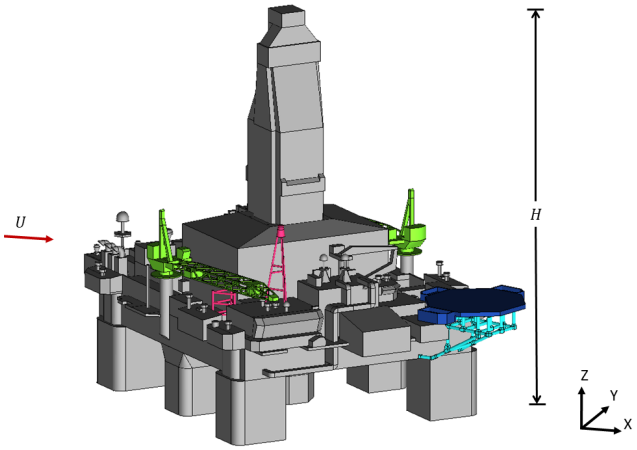

Figure 2: CAD Model of Offshore Platform.

It is evident from the geometry of the offshore platform in Figure 2, that when the wind direction is such that the helideck is in the lee of the drilling derrick, the air flow over and around the helideck will be turbulent due to separation of the flow from the large upstream superstructures, particularly the clad derrick. Winds approaching the rig which put the helideck downstream of the derrick are therefore more likely to present a challenging environment in which the helicopter pilot must operate during take-off and landing (launch and recovery). To assess the effect of the disturbed air flow on the helicopter and on pilot workload, the airwake was computed with the rectangular geometry of the platform positioned at 45° to the oncoming wind, U, with the helideck downstream of the derrick.

2.1 Time-accurate CFD Method

To adequately model the offshore platform's airwake for piloted flight simulation, particularly in terms of helicopter handling qualities and pilot workload, a time-accurate CFD approach is required [19]. The irregular time-varying velocities in the computed airwake will

then be applied to the aircraft flight dynamics model in the simulation to create the unsteady loads on the aircraft, which the pilot will experience.

DDES is a time-accurate CFD method suitable for modelling unsteady flow dominated by both quasi-periodic large-scale structures and chaotic small-scale turbulent features typical of bluff body geometries [20]. Similar computational methods have been previously used to model ship airwakes for aircraft flight simulation and have been validated against experimental measurements for both frigates [21] and aircraft carriers [22]. DDES uses a hybrid approach to turbulence modelling where Large Eddy Simulation, LES, is used away from the surfaces of the platform to directly resolve the larger-scale turbulent structures, while unsteady Reynolds-averaged Navier–Stokes, URANS, is applied closer to the surface [23]. The DDES airwake analysis was carried out using ANSYS Fluent with a Shear Stress Transport k–ω based turbulence model and third order accuracy momentum discretization. This hybrid method of computation is particularly suited to airwake modelling of the offshore platform as in regions of interest, such as over the helideck, the turbulent features of the flow are explicitly resolved with a reduction in computational time required compared with 'pure' LES. Also, when compared with a 'pure' URANS approach, DDES produces less dissipation of turbulent kinetic energy in the flow shed from the bluff superstructure. To adequately resolve the turbulent length scales within the airwake over the helideck using LES, and to reduce artificial dissipation, it is necessary for the mesh size in the CFD region of interest, or 'focus region', to be sufficiently refined. Grid generation over the helideck was therefore carefully controlled to maintain a sufficiently dense mesh.

The offshore platform model, Figure 2, was placed in a rectangular domain 15 H long, 9 H wide and 5 H high. The cell size at the surface of the offshore platform was set at 0.35 m. Twelve prism layers were applied on the non-slip surfaces. Using a non-dimensionalised first layer height y^+ of 30 and a growth ratio of 1.2, the height of the next layer was calculated using the exponential prism growth law. The resulting total unstructured mesh size, including the more dense focus region over the flight deck, was about 50 million cells. At the inlet to the CFD domain, a velocity profile was applied to represent an oceanic atmospheric boundary layer, ABL, using Equation 1, where U_{ref} is the reference windspeed measured at a known height above sea-level, z_{ref}, and z_0 is the sea-surface roughness length-scale which can be taken as 0.001 m for oceanic conditions, according to Garratt [24].

$$U = U_{ref}\left(\frac{ln(\frac{z}{z_0})}{ln(\frac{z_{ref}}{z_0})}\right) \quad (1)$$

Each surface of the offshore platform was modelled as a zero-slip wall. The sides and top of the rectangular domain were set as symmetry walls and the outlet was set as a pressure outlet. The sea-surface of the domain was set as a slip wall, thereby allowing the prescribed ABL to be maintained throughout the domain. The reference wind speed, U_{ref}, was set to a value of 40 kt (20.6 m/s) at a reference height, z_{ref}, of 44 m above the sea surface, which is close to the height of the main rotor during hover above the flight deck. Figure 3 shows the computed airwake with the derrick at a 45° angle, to the oncoming wind direction, which is in the x-y plane. The airwake is shown as contours of u-velocity normalised by U_{ref} and the vertical plane is through the centre of the drilling derrick. Also included in Figure 3 is the ABL velocity profile applied to the inlet of the domain and the location of z_{ref} shown as a horizontal red line. An initial steady solution was computed using RANS. The solver was then switched to DDES and allowed to run for a settling period of 20 seconds before 30 seconds of unsteady data were recorded. The total solution was computed over 5 days on 128 parallel nodes.

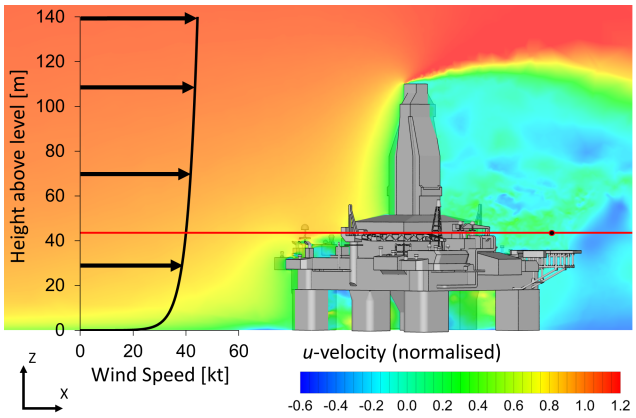

Figure 3: Contours of normalised u-velocity in a plane through the centre of the main derrick, including the ABL inlet profile.

Figure 4 shows the vortical structures in the CFD-generated airwake, illustrated using the Q-criterion vortex identification method [25], as iso-surfaces of vorticity coloured by instantaneous streamwise u-velocity. It can be seen that the helideck in the lee of the derrick is immersed in highly turbulent air flow.

Figure 5 shows contours of mean velocity magnitude, normalised by U_{ref}, in a horizontal plane 20 ft above the helideck, which is approximately the height of the helicopter centre of gravity when the main rotor is at about 25 ft above the deck. The outline of the helideck is also shown in Figure 5, with the landing spot at it's centre. A large region of separated flow, or wake, is observed in the lee of the drilling derrick with a reduction in the velocity magnitude over the helideck varying between 20% and 70% of the freestream ve-

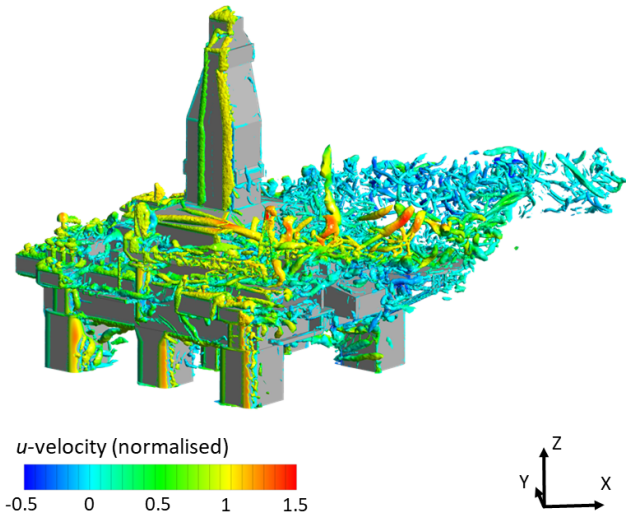

Figure 4: Airwake over the offshore platform presented as instantaneous isosurfaces of Q-criterion coloured by normalised u-velocity.

locity. Velocity differentials of this magnitude can create significant aerodynamic forces and moments on the aircraft, particularly when the helicopter is over the helideck during launch and recovery.

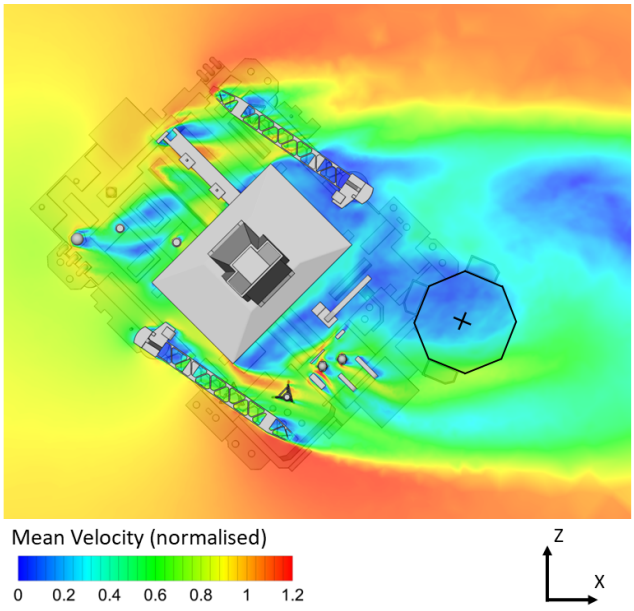

Figure 5: Contours of mean velocity magnitude in a vertical plane 20 ft above the helideck.

Figure 6 shows contours of instantaneous velocity magnitude, normalised by U_{ref}, again in a horizontal plane 20 ft above the helideck. The instantaneous image of the flow in this plane highlights the spatial variation of velocity in the region over the helideck. At this particular instant in time, a region of high velocity flow of approximately 110% of the freestream velocity magnitude is observed at the edge of the helideck, showing that the velocity differentials that can lead to aerodynamic forces and moments on the aircraft will be transient and will add to the pilot's workload when attempting to control the aircraft.

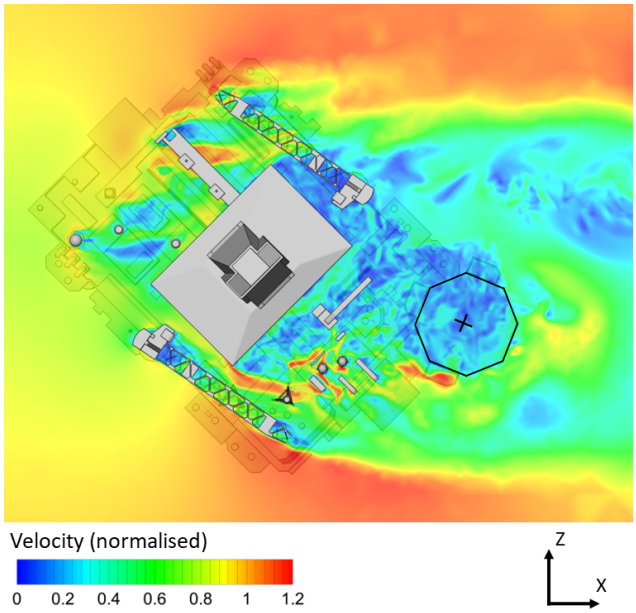

Figure 6: Contours of instantaneous velocity magnitude in a vertical plane 20 ft above the helideck.

Figure 7 shows contours of turbulence intensity in a horizontal plane 20 ft above the helideck. Turbulence intensity, T_i, is defined as the Root Mean Square, RMS, of the turbulent velocity fluctuations divided by the freestream flow velocity, i.e. not the local velocity, and is calculated using Equation 2, where u', v', w' are the fluctuations in the three velocity components u, v, w.

$$T_i = \frac{\sqrt{\frac{1}{3}(u'^2 + v'^2 + w'^2)}}{U_{ref}} \quad (2)$$

Figure 13 shows that in this wind condition, the platform structure, particularly the lower section of the derrick, generates a large turbulent wake; the red areas, with turbulence of about 25% are the unsteady shear layers formed by the air flow separating from the vertical edges of the structure. The air flow above the helideck can be seen to have about two-thirds of its area exposed to air with a turbulence intensity of about 10% with the remainder of the deck in an air flow with a turbulence intensity of about 25%. These turbulence levels, and the uneven distribution, will again induce unsteady aerodynamic loads on the aircraft and, to add to the complexity, the distinct turbulent areas will themselves be moving around in the unsteady flow. These high values and spatial variations of turbulence intensity over the helideck can be expected to challenge the

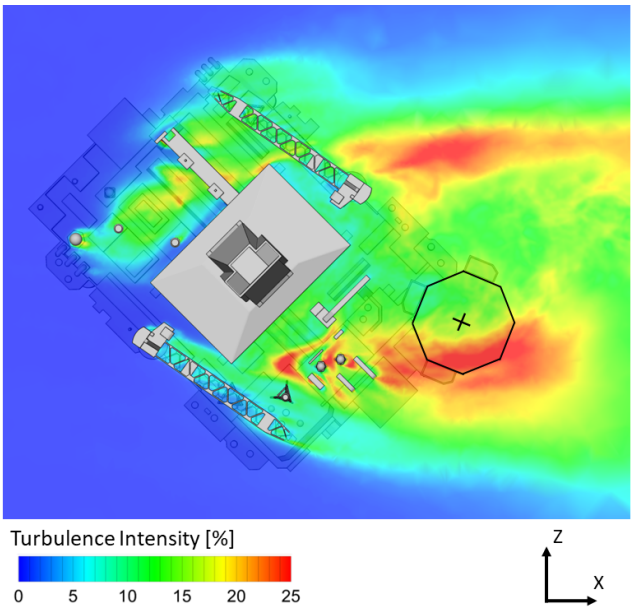

Figure 7: Contours of turbulence intensity in a vertical plane 20 ft above the helideck.

pilots during helicopter launch and recovery.

To further illustrate the unsteady nature of the flow, Figure 8 shows the vertical velocity component, w, at a point 20 ft above the landing spot. For a 40 kt wind the vertical component fluctuates between about −9 m/s to +6 m/s. Such fluctuations will be present in all three velocity components and they will vary significantly throughout the airwake. It is therefore not surprising that turbulence is a major factor when flying over the helideck and that its inclusion in the simulation is essential.

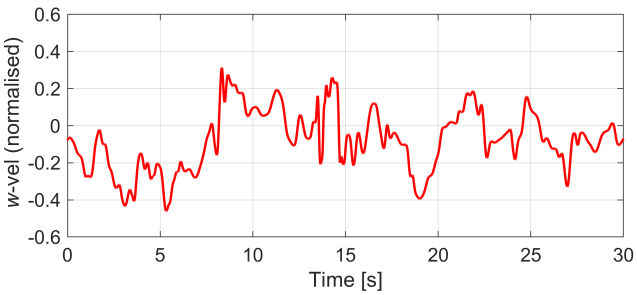

Figure 8: Computed w-velocity at 20 ft above the centre of the helideck.

3 Piloted Flight Simulation

To assess the effect of the offshore platform's airwake on the helicopter and on pilot workload during recovery to the helideck, a piloted flight trial was conducted within a simulated environment. The HELIFLIGHT-R fully reconfigurable research simulator [26], shown on the left of Figure 9, has been used in several studies to investigate the effects of CFD-generated ship airwakes on a helicopter and on pilot workload experienced during simulated at-sea deck landings [27–29]. The twin-seat generic rotorcraft cockpit is housed within a 12 ft diameter visual display dome mounted on a standard hexapod motion platform with six electric 24 inch stroke actuators. A third seat is available to the rear of the cabin for an instructor or simulator operator. Two wide-screen monitors provide the primary cockpit instrument panels and allow straightforward reconfiguration for each simulated aircraft. The force-feel characteristics of the cyclic, collective and pedal controls can also be reconfigured to represent a wide range of aircraft types due to a four-axis electronic control loading system. Four Digital Light Processing projectors, each with a resolution of 2,560 × 1,600 pixels, project the outside world image from the view of the cockpit onto the inside surface of the dome, as can be seen on the right of Figure 9. The projectors provide a vertical field-of-view of 100° (+30°/-70°) and a horizontal field-of-view of 230° (+120°/-110°). Audio cues are provided to the pilot via loudspeakers distributed throughout the cabin.

Figure 9: Visual Environment in the HELIFLIGHT-R flight simulator.

A generic rotorcraft flight dynamics model, configured to represent a SH-60B Seahawk using Advanced Rotorcraft Technology's FLIGHTLAB software [30], was integrated with the HELIFLIGHT-R simulator. Although it is recognised that the Seahawk helicopter is not typically used in the offshore industry, this aircraft model was used in this 'proof-of-concept' exploratory flight trial, due the strong validation data available [31] and its extensive use in previous ship airwake simulation research at the University of Liverpool [16,27–29]. The helicopter flight dynamics model within FLIGHTLAB applies the local time-varying three-dimensional velocity components to airload computation points, ACPs, at various locations on the rotor blades and airframe, thereby allowing the CFD-generated airwakes to interact with the aircraft's aerodynamic model. A vi-

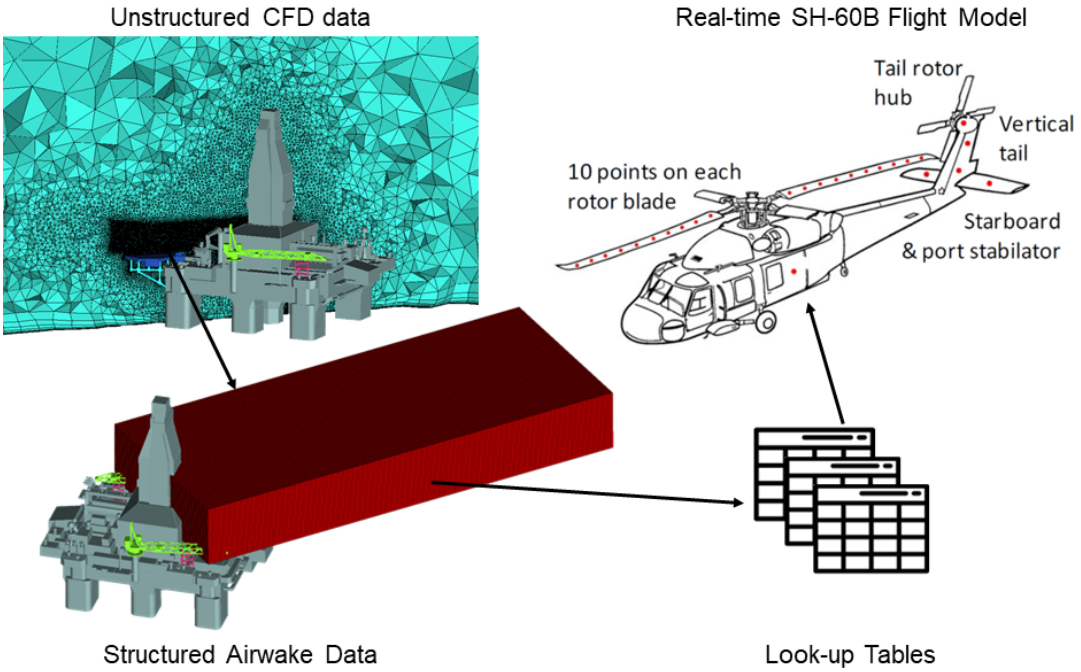

Figure 10: Integration of CFD airwake with helicopter flight dynamics model.

sual model of the offshore platform was created using PRESAGIS software and integrated into the simulator run-time environment to provide the pilot with an appropriate visual scene generated. Thirty seconds of computed unsteady three-dimensional velocity components were looped within the simulation to provide a sustained airwake. During the trial, real-time flight data is monitored and recorded through FLIGHTLAB which, together with recordings of the audio and visual scene, are used for post-trial analysis.

The method by which the unsteady airwake is integrated with the representative Seahawk flight dynamics model is illustrated in Figure 10. Due to the complex geometry of the offshore platform, an unstructured mesh was generated to solve the flow, as shown in the top left of Figure 10 (which also shows the dense focus region over the helideck). The air flow is computed on the unstructured mesh at 100 Hz for 30 seconds. As the region in which the aircraft will be operating during the flight trial is known, and to reduce the airwake size, the time-dependent velocity components from the unstructured mesh are interpolated onto a structured grid and down-sampled to 25 Hz. The structured grid, extending downwind of the derrick and over the helideck is shown in the bottom left of Figure 10. The volume of the structured grid also incorporates the approach path used in the trials, which was with the aircraft facing into the oncoming freestream wind direction and aligned with the landing spot at the centre of the helideck. The volume containing the structured grid measured 240 m by 100 m by 33 m, with a grid spacing of 1 m.

The interpolated velocity data of the airwake is converted into lookup tables in Simulink to be read into FLIGHTLAB and integrated with the helicopter flight model. As described above, the airwake was computed for a wind speed, U_{ref}, of 40 kt (20.6 m/s). The flight trials were conducted for freestream wind speeds of 20, 30, 40 and 50 kt and the velocities within the 40 kt airwake were therefore scaled accordingly for each wind speed. The scaling was carried out by multiplying each velocity component at every location in the airwake and at every time step by the appropriate factor (e.g. for the 20 kt wind the 40 kt velocities were halved) and, when the airwakes were run in the simulator, the speed at which the files were played was also linearly scaled (e.g. for the 20 kt airwake the 40 kt airwakes were run at half speed). This method of scaling is possible because the overall flow topology is Reynolds number independent, and the shedding frequency at different wind speeds follows Strouhal scaling. The validity of the scaling method has been previously demonstrated for ship airwakes in [32]. The airwake for each wind speed therefore had its own lookup table so the unsteady air velocities could be applied to the helicopter ACPs in real time within FLIGHTLAB as the helicopter moves around within the airwake; as the aircraft has no effect on the airwake, this integration is known as one-way coupling. The 30 seconds of computed airwake are looped to provide continuous flow during flight simulation. The image in the top right of Figure 10 shows the distribution of the 46 ACPs on the SH-60B helicopter flight dynamics model. Ten ACPs are located along each of the four main rotor blades, with one at the centre of gravity, one on each of the port and starboard stabilisers, two on the verti-

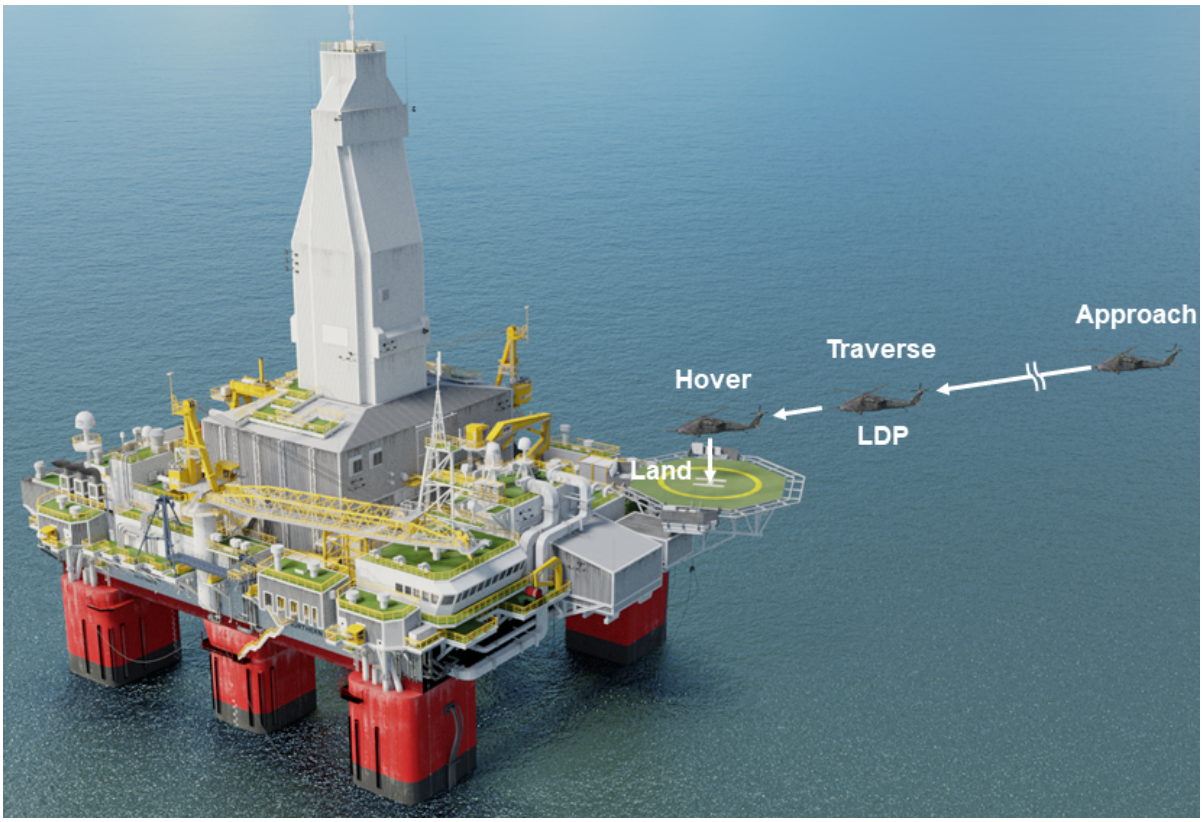

Figure 11: Helicopter Recovery Approach to the Offshore Platform.

cal tail and one at the tail rotor. Previous investigations into the effect of ship airwakes on helicopter operations have been conducted using the integration method described above [27–29].

During the simulated flight trial, a helicopter test pilot with extensive experience in operating to offshore platforms, was instructed to perform a recovery to the helideck at freestream wind speeds of 20, 30, 40 and 50 kt. The pilot performed an approach, which is illustrated in Figure 11, starting from 3400 ft out, flying directly into (freestream) wind at a 0° heading on a trajectory aligned with the centre of the helideck. The overall manoeuvre was split into four mission task elements, MTEs, also illustrated in Figure 11. The first MTE is the approach from the initial position 3400 ft downwind of the helideck at a height of 500 ft above sea level to the Landing Decision Point, LDP, which is 150 ft above sea level approximately one rotor diameter from the front of helideck. The LDP is the point where the pilot must commit to the landing and be able to land on the helideck in the event of critical engine failure [33, 34]. The second MTE requires the pilot to traverse the helicopter from the LDP across the helideck and assume a position 20 ft above the landing spot. For MTE 3 the pilot must maintain hover over the landing spot for 30 seconds at a heading of 0° with a 'desired' yaw of ±5° and height of ±3 ft; 'adequate' limits are defined as ±10° in yaw and ±5 ft in height. Finally, the 4th MTE is the descent from the hover position, where the pilot should attempt to safely touchdown the aircraft at the designated landing spot at a heading of 0° with a desired yaw of ±5° and within ±1.5 ft of the spot; adequate limits are defined as ±10° in heading and ±3 ft in position. The difficulty of the recovery task was assessed by the test pilot using three subjective ratings scales: a workload rating was assigned to each MTE from the Bedford workload rating scale [35], the intensity of turbulence was given for each MTE from the turbulence rating scale [36], and a rating from the Deck Interface Pilot Effort, DIPES, scale [37] was given for the whole task. The three scales are shown in Figures 12, 13, and 14 respectively.

The pilot's perceived workload, based on the level of spare capacity they have to perform additional tasks, was assessed using the Bedford workload rating scale shown in Figure 12, where workload is defined as the integrated physical and mental effort generated by the perceived demands of a specified piloting task [35]. After each MTE task, the pilot assesses their level of spare capacity and assigns a rating from the ten-point Bedford workload scale. A rating of 1-3 will be awarded if the workload is satisfactory during the task. Where the workload is unsatisfactory and reduced the pilot's capacity to perform additional task, a rating of 4-6 will be awarded. Ratings of 7-9 indicate that while the

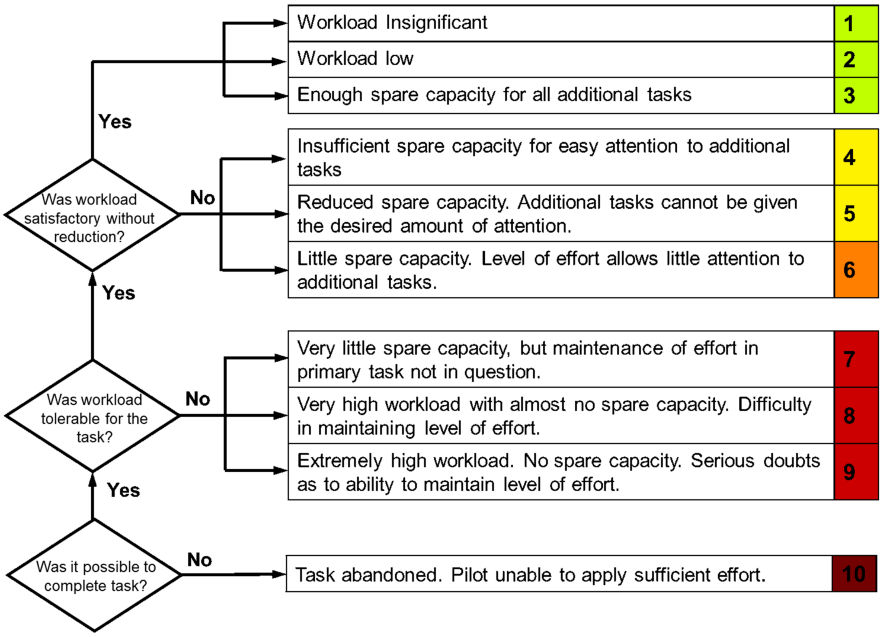

Figure 12: Bedford workload rating scale [35].

INTENSITY	AIRCRAFT REACTION	REACTION INSIDE AIRCRAFT
LIGHT		
Turbulence	Turbulence that momentarily causes slight, erratic changes in altitude and/or attitude (pitch, roll, yaw).	Occupants may feel a slight strain against seat belts or shoulder straps. Unsecured objects may be displaced slightly. Food service may be conducted and little or no difficulty is encountered in walking.
Chop	Turbulence that causes slight, rapid and somewhat rhythmic bumpiness without appreciable changes in altitude or attitude.	
MODERATE		
Turbulence	Turbulence that causes changes in altitude and/or attitude occur but the aircraft remains in positive control at all times. It usually causes variations in indicated airspeed.	Occupants feel definite strains against seat belts or shoulder straps. Unsecured objects are dislodged. Food service and walking are difficult.
Chop	Turbulence that causes rapid bumps or jolts without appreciable changes in aircraft altitude or attitude.	
SEVERE		
Turbulence	Turbulence that causes large, abrupt changes in altitude and/or attitude. It usually causes large variations in indicated airspeed. Aircraft may be momentarily out of control.	Occupants are forced violently against seat belts or shoulder straps. Unsecured objects are tossed about. Food Service and walking are impossible.
EXTREME		
Turbulence	Turbulence in which the aircraft is violently tossed about and is practically impossible to control. It may cause structural damage.	

Figure 13: Turbulence rating scale [36].

task can be performed successfully, the workload was regarded as intolerable. If the pilot is unable to complete the task and it is abandoned due to high workload, a rating of 10 will be awarded.

The turbulence rating scale is used by pilots to report conditions to Air Traffic Control when encountering turbulence. As shown in Figure 13, the turbulence ratings scale has four levels that the pilot may award depending on the intensity of turbulence experienced. Light turbulence is defined as ‘turbulence that momentarily causes slight erratic changes in altitude and/or attitude (pitch, roll, yaw)’. A rating of moderate is given when the turbulence is of greater intensity than light turbulence where ‘changes in altitude and/or attitude occur but the aircraft remains in positive control at all times’. Severe turbulence is defined as turbulence that causes ‘large, abrupt changes in altitude and/or attitude with large variations in indicated airspeed resulting in the aircraft being momentarily out of control’. A rating of extreme turbulence is given when the aircraft is ‘violently tossed about, is practically impossible to control, and may result in structural damage to the aircraft’.

The recovery of maritime helicopters to ships at sea

EFFORT	GUIDANCE	DIPES
Slight to Moderate	Reasonable compensation required. Tracking and positioning accuracy is consistently maintained throughout the operation. Fleet pilots will have enough spare capacity to conduct ancillary tasks.	**1**
Considerable	Significant compensation required. Tracking and positioning accuracy occasionally degrades during peaks in ship motion, sea spray or turbulence. Fleet pilots will have difficulty conducting ancillary tasks.	**2**
Highest Tolerable	Highest tolerable compensation required. Tracking and positioning accuracy degrades regularly during peaks in ship motion, sea spray or turbulence. Fleet pilots will be able to keep up with task requirements but no more. Degraded operations (ship or aircraft) will probably require an abort. Repeated safe operations are achievable. This point defines the recommended limit.	**3**
Excessive	Excessive compensation required. Accuracy is poor in one or more axes. Fleet pilots will be purely reacting to external influences rather than anticipating them. A safe abort may not be possible if an aircraft or ship system is lost during a critical phase of the evolution. Fleet pilots under operational conditions could not consistently repeat these evolutions safely.	**4**
Dangerous	Extreme compensation required. Repeated safe evolutions are not possible even under controlled test conditions with fully proficient crews.	**5**

Acceptable DIPES 1-3	Unacceptable DIPES 4-5

Note: Each DIPES rating may be given one or more suffixes to describe the cause(s) of the increased workload.

Pitch control:	P	Height control:	H
Turbulence:	T	Spray:	S
Roll control:	R	F/Aft positioning:	F
Deck motion:	D	Torque control:	Q
Yaw control:	Y	Lateral positioning:	L
Visual cues:	V	Funnel exhaust:	E
A/C attitude	A		

Figure 14: DIPES rating scale [37].

encounter similar challenges to helicopter recovery to the helideck of an offshore platform, with the added challenge of a moving landing deck. The helicopter pilot in both instances often has to contend with the unsteady airwake generated by upstream superstructures. To reduce the risk to the helicopter and pilot, operational limits are defined for each ship-aircraft combination. For naval ships, such limits are determined by NATO member countries by conducting flight trials and using the DIPES rating scale, which assesses the difficulty of the overall landing task [37]. Unlike the Bedford scale, which focuses on pilot workload, the DIPES also accounts for the aircraft physical control margins and identifies environmental factors such as turbulence. While it is recognised that DIPES is not typically used for assessing the difficulty of helicopter operations to an offshore platform, DIPES was used in this study due to its suitability for qualification testing where, although pilot workload may be low, aircraft control limits can be encountered. Figure 14 shows the five-point DIPES scale used to assess the difficulty of the complete launch/recovery task. A DIPES rating of 1-3 ranks effort from slight to the highest tolerable while still being considered within acceptable bounds and the capabilities of an average fleet pilot. A rating of 4 is given if the assessing pilot deems the task to be unacceptable on the basis that an average fleet pilot would not be able to complete the task in a consistently safe manner. If the task cannot be safely completed by fully proficient crews, even under controlled test conditions, a rating of 5 is awarded.

During the simulated flight trials, the pilot was asked to award Bedford workload and turbulence ratings for each MTE of the helicopter recovery task. After completion of the recovery, a DIPES rating was awarded and any pilot comments documented. Flight simulation test data was recorded for each recovery task in FLIGHTLAB, including the pilot inputs to cyclic, collective and pedals controls, as well as aircraft position, attitude and accelerations in six degrees of freedom. The airwake velocity components were also recorded during the recovery task at each of the 46 ACPs within the flight dynamics model.

4 Flight Trial Results

A selection of results from the flight trial are presented and discussed in the following sections, beginning with the pilot's assessments using the three rating scales, followed by recordings of the aircraft yaw and altitude and, finally, the associated input activity in the cyclic control during the hover MTE.

4.1 Pilot Ratings for Recovery Task

Table 1 presents the Bedford workload ratings awarded for each MTE and the overall DIPES ratings when landing to the helideck at wind speeds of 20, 30, 40 and 50 kt. For all wind speeds, during MTE 1 the workload was deemed to be satisfactory. For the remainder of the recovery task, in a 20 kt wind, the workload was tolerable but was not satisfactory without a reduction in spare capacity. A DIPES rating of 2 was awarded for the whole recovery task in the 20 kt wind, which indicates that significant compensation

was required by the pilot. On completion of the recovery task, the pilot commented that *"the modelling does feel quite real"* providing confidence in the simulation fidelity. In the 30 kt wind condition, for MTE 2 the pilot awarded a Bedford workload rating of 6, indicating that the workload resulted in little available spare capacity and attention for additional tasks. Bedford ratings of 7 were awarded for MTEs 3 and 4 in the 30 kt wind, indicating the workload was deemed intolerable by the pilot with very little spare capacity available; however, the maintenance of effort on the primary task was not in question, leading to an overall DIPES rating of 3 which indicates that the effort required for the task was the highest tolerable for the average fleet pilot. Similar workload ratings were given for MTEs 2 to 4 in the 40 and 50 kt winds and show an increase in workload from those given for a 30 kt wind. MTE 3 saw the highest workload in the trial with a rating of 9, indicating extremely high workload with no spare capacity and serious doubts as to the ability to maintain level of effort. The pilot, after completing the recovery in a 40 kt wind, stated that the modelling *"felt very life-like"* and that they had *"flown to similarly cladded deck and it* [the airwake] *felt like that"*. The DIPES ratings of 4 given for 40 and 50 kt indicate that operations by an average fleet pilot would be inconsistently safe as excessive compensation would be required.

For each wind speed in Table 1, the approach to the offshore platform (MTE 1) resulted in low pilot workload, which is consistent with the lower turbulence intensity values observed in Figure 7. Transitioning from the LDP to over the helideck results in higher workload ratings; this is consistent with the aircraft entering the region of high turbulence intensity shown in Figure 7. The maximum workload ratings are given for the translation, hover and landing MTEs. The increase in workload ratings awarded for MTEs 2 to 4 is consistent with the conventional view of the CAA that the greatest risk to helicopter operations is at the point at where the helicopter arrives over the helideck and is required to hover prior to touchdown [3]. Figure 5 and 7 show that, at hover height, the main rotor will pass through two distinct flow regions: one with a low mean velocity and low turbulence close to the centre of the helideck and a second region with relatively high mean flow velocity and high turbulence towards the edge of the helideck. Such velocity differentials can be expected to create unsteady loads on the aircraft.

The overall DIPES ratings given by the pilot during the simulated flight trial, shown in Table 1, specify that in the applied wind condition the maximum wind speed that a pilot would be able to consistently operate safely is 30 kt. This maximum allowable wind speed may be increased with further recovery manoeuvres performed at varying incremental wind speeds between 30 and 40 kt. Overall the level of simulation fidelity provided by the time-accurate unsteady airwake was well received by the pilot.

Table 1: Bedford workload and DIPES ratings.

Wind, kt	Bedford workload ratings				DIPES
	MTE 1	MTE 2	MTE 3	MTE 4	
20	3	4	5	5	2
30	2	6	7	7	3
40	2	8	9	8	4
50	3	8	9	8	4

Table 2 shows the turbulence ratings given by the pilot for winds from 20 to 50 kt for each MTE of the recovery task. At 20 and 30 kt the pilot experienced low or no turbulence until nearing the edge of the flight deck at the LDP, where moderate turbulence was experienced for the remaining recovery manoeuvre. The pilot mentioned that the moderate turbulence rating was due to the *"potentially large"* turbulence disturbances. The turbulence ratings for 20 and 30 kt are consistent with the DIPES ratings shown in Table 1 as moderate turbulence is defined as the aircraft remaining in positive control at all times. At 40 and 50 kt, the turbulence rating for MTEs 2 to 4 increased from moderate to severe, indicating that the turbulence was causing large, abrupt changes in altitude and/or attitude and possible large variations in airspeed which may have resulted in the aircraft being momentarily out of control. The corresponding DIPES ratings for 40 and 50 kt in Table 1 gave unacceptable levels of compensation, which is consistent with severe turbulence.

Table 2: Turbulence ratings.

Wind, kt	Turbulence Rating			
	MTE 1	MTE 2	MTE 3	MTE 4
20	N/A	Moderate	Moderate	Moderate
30	Light	Moderate	Moderate	Moderate
40	Light	Severe	Severe	Severe
50	Light	Severe	Severe	Severe

4.2 Aircraft Yaw and Height During Recovery Task

Figure 15 shows the aircraft yaw during the complete recovery task in each wind speed. In the graph, the time histories are split by two vertical dotted lines which represent the start and end of the 30-second hover task (MTE 3). The traverse task, MTE 2, was initialized by the pilot after reaching the LDP, approximately 45-30 seconds before the start of the hover task. The point at which the LDP was reached for each wind speed is marked with a diamond symbol on each time history. The two horizontal dashed lines show

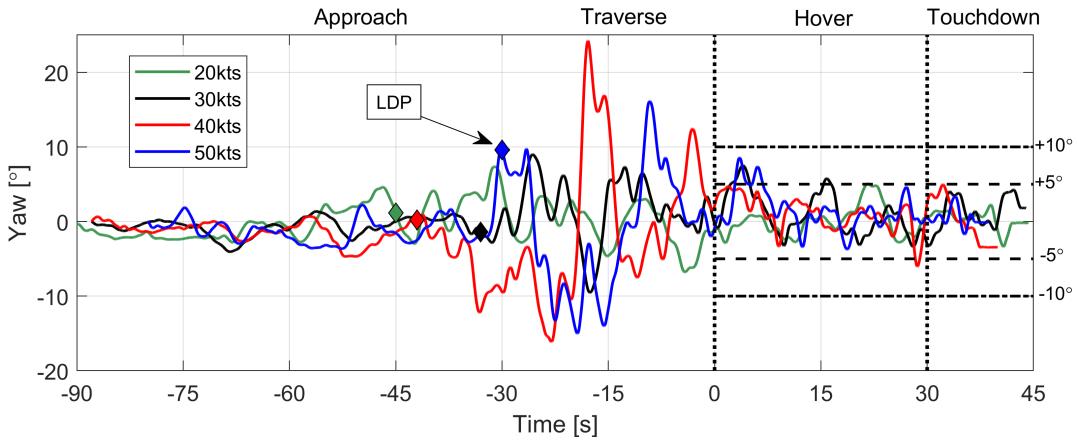

Figure 15: Helicopter yaw during recovery.

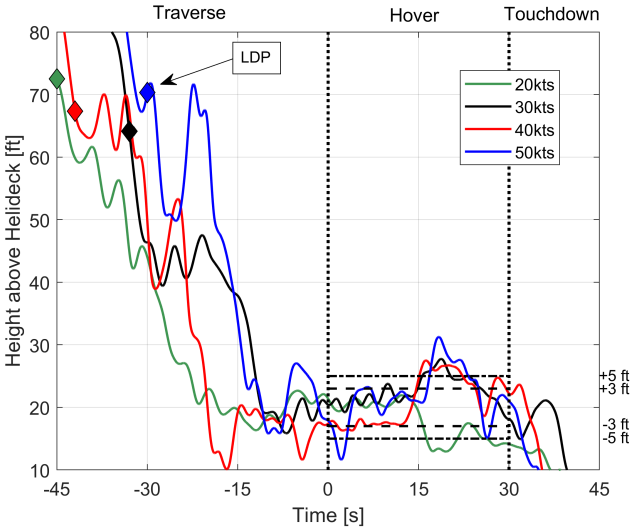

Figure 16: Helicopter height above helideck during recovery.

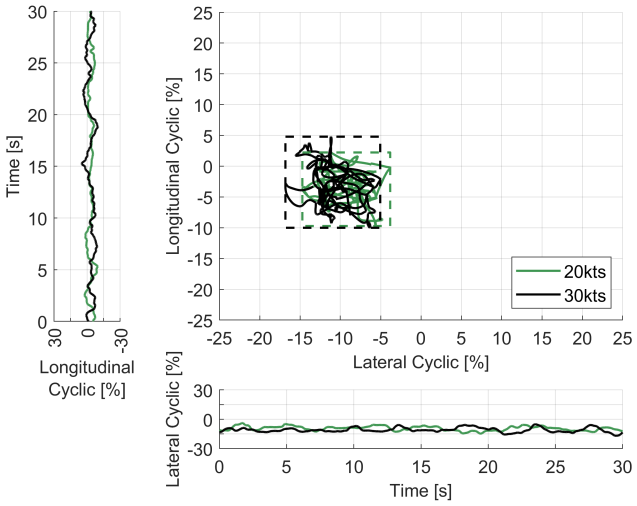

Figure 17: Longitudinal and lateral cyclic inputs during hover at 20 kt and 30 kt.

the maximum/minimum desired yaw ±5° at a heading of 0° required during the hover and touchdown task elements of the recovery. Similarly, the two horizontal dot-dashed lines indicate the maximum/minimum adequate yaw of ±10° during the final two MTEs. For the approach, MTE 1, it can be seen that for all wind speeds there is not a large variation in aircraft yaw, which is consistent with the low Bedford workload ratings awarded in Table 1, and with the low levels of turbulence some distance downstream of the helideck, shown in Table 2. However, as the helicopter approaches the helideck, indicated by the LDP symbols in Figure 15, the deviations in yaw becomes more erratic, particularly at the higher wind speeds, and is again consistent with the increased workload ratings awarded for the Traverse, MTE 2, and with the high turbulence intensities close to and over the helideck, shown in Figure 7 and reflected in Table 2. During the hover task, MTE 3, the pilot was able to maintain yaw within the adequate bounds for each wind speed and within the desired bounds at 20 kt; however, the pilot commented that they had *"difficulty in maintaining yaw and height"*. During the touchdown, MTE 4, the pilot was able to maintain the aircraft within the bounds of desired for each wind speed but, as indicated by the high ratings awarded for MTEs 3 and 4 in Table 1, the pilot considered the workload to be intolerable and, as shown in Table 2, the turbulence to be severe.

Figure 16 shows the helicopter height during the complete recovery task in each wind speed. As in Figure 15, the time histories are split by two vertical dotted lines that represent the start and end of the 30-second hover task; the LDP is again marked by diamond symbols. Similarly, the two horizontal dashed lines show the maximum/minimum desired height of ±3 ft required during the hover MTE, and the dot-dashed lines show the maximum/minimum adequate height of ±5 ft. The increased variations in aircraft altitude as the pilot passes through the LDP and begins

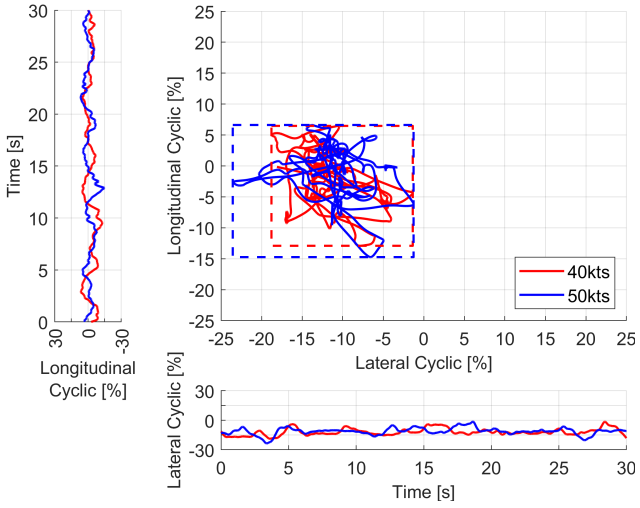

Figure 18: Longitudinal and lateral cyclic inputs during hover at 40 kt and 50 kt.

the traverse to the hover position is consistent with the variations in yaw for the same MTE shown in Figure 15 and is due to the aircraft encountering the turbulent airwake close to and over the helideck. During the hover MTE, Figure 16 shows that the pilot was unable to maintain the desired, or even the adequate height for all wind speeds and they commented that as the helicopter came over the flight deck *"you could feel the updraft and downdraft"* resulting in over-control of the collective to try and maintain height (consistent with the positive and negative vertical velocities shown earlier in Figure 8). Again, the reason for the difficulty the pilot experienced in holding height is due to the airwake over the flight deck, shown in Figure 7 and reflected in Table 2.

4.3 Cyclic Control Activity During the Hover Task

Figures 17 and 18 show the pilot's cyclic control activity during the hover task, MTE 3, where the pilot was asked to hold position for 30 seconds over the landing spot at the centre of the helideck. The central graph in each figure shows the lateral/longitudinal cyclic displacement, while the outer time-based graphs show how the lateral and longitudinal inputs changed with time. To highlight the level of cyclic control activity, a broken-line box has been used to bound the maximum displacement of each dataset. Figure 17 shows the cyclic inputs for the 20 and 30 kt winds during the hover task. An increase can be seen in the maximum displacement from the held cyclic position in the higher wind speed of 30 kt. The cyclic inputs recorded during the hover task in a 40 and 50 kt wind are shown in Figure 18 and, consistent with the data shown in Figure 17, larger displacements from the held cyclic position, both laterally and longitudinally, are observed at higher wind speeds. The increase in control activity with wind speed is consistent with the workload ratings provided by the pilot for the hover task, the overall DIPES ratings provided in Table 1, and the turbulence level ratings given in Table 2. As in the discussions above, the increased control activity in hover is because the aircraft is immersed in the turbulent airwake over the flight deck and the magnitude of the fluctuations and differentials in the air velocities increase with wind speed.

5 Conclusions

This paper has described a study in which piloted flight simulation has been used to investigate the effect of an offshore platform's unsteady airwake on the helicopter and pilot workload during helideck landings. Overall, the piloted flight trial was deemed successful and was considered by the pilot to be representative of the real-world experience. This positive outcome opens up the possibility that piloted flight simulation could be used to provide training, or experience, for helicopter pilots before they fly to an offshore platform. Furthermore, it is not an unrealistic proposition that simulation could be used to explore different approaches to platforms at different wind conditions to identify the safest method for helicopter launch and recovery.

The main conclusions are as follows:

- Time-accurate CFD showed the presence of a large unsteady airwake being generated by the offshore platform's superstructure, resulting in areas of low mean flow velocity and two large shear layers with high levels of turbulence intensity.
- The level of simulation fidelity provided by the time-accurate unsteady airwake was well received by the pilot who commented that the turbulent airwake *"felt very lifelike"*.
- During the approach task of recovery to the helideck the workload rating was low with a turbulence rating of 'no to light' for wind speeds of 20 – 50 kt.
- The study has shown conclusively that the aircraft and pilot are most affected when the aircraft approaches the helideck and enters the highly turbulent airwake created by the platform structure.
- The overall DIPES ratings given by the pilot during the simulated flight trial determined that in the assumed wind direction, the maximum wind speed in which a pilot would be able to consistently operate safely, is 30 kt.
- Aircraft heading was maintained within the bounds of adequate for 30, 40 and 50 kt and within

desired for 20 kt; however, there were large variations in heading during the traverse to the helideck due to the airwake.

- Aircraft height bounds of adequate were exceeded during hover over the landing spot for wind speeds of 20 to 50 kt, again due to the turbulent air flow over the helideck.

- Similarly, increasing wind speed resulted in an increase in cyclic control activity during the hover task above the helideck indicating that the pilot was finding it difficult to hold the aircraft in both yaw and altitude.

Acknowledgements

The authors would like to acknowledge the ongoing support of ANSYS UK. They would also like to thank Dr Christopher Dadswell from the Flight Science and Technology research group at the University of Liverpool for his expertise.

References

[1] "CAP 437 - Standards for offshore helicopter landing areas," Tech. rep., UK Civil Aviation Authority, June 2021, 8th edition.

[2] Lorette Fabre Photographe/Airbus, Available at https://www.airbus.com/en/products-services/helicopters/hcare-services/training-flight-operations/maintenance-training, Accessed: February 2022.

[3] "CAA Paper 99004 - Research on Offshore Helideck Environmental Issues," Tech. rep., UK Civil Aviation Authority, 2000.

[4] "Helicopter Limitations List (HLL)," Tech. rep., Helideck Certification Authority, August 2022, HLL Issue - 04.

[5] "CAA Paper 2008/03 Helideck Design Considerations - Environmental Effects," Tech. rep., UK Civil Aviation Authority, July 2009.

[6] "NOROSK C-004 Helicopter deck on offshore installations," Tech. rep., NORSOK, October 2019.

[7] Mentzoni, F., Ertesvåg, I. S., Rian, K. E., and Kleiveland, R. N., "Numerical modeling of turbulence above offshore helideck – Comparison of different turbulence models," *Journal of Wind and Industrial Engineering*, Vol. 141, 2015, pp. 49–68.

[8] Mentzoni, F. and Ertesvåg, I. S., "On turbulence criteria and model requirements for numerical simulation of turbulent flows above offshore helidecks," *Journal of Wind and Industrial Engineering*, Vol. 142, 2015, pp. 164–172.

[9] Colognato, F. and Scala, S., "Wind Characterisation Around Offshore Platform for Real-time Helicopter Simulator," 43rd European Rotorcraft Forum, Milan, Italy, 12-15th September 2017.

[10] Stickland, M., Fabre, S., Scanlon, T., Oldroyd, A., Mickelson, T., and Astrup, P., "CFD Technique for Estimating Flow Distortion Effects on Lidar Measurements When Made in Complex Flow Fields," *Engineering Applications of Computational Fluid Mechanics*, Vol. 7, No. 3, 2013, pp. 324–333.

[11] de Carvalho e Silva, D. F., Pagot, P. R., Nader, G., and Jabardo, P. J. S., "CFD Simulation and Wind Tunnel Investigation of a FPSO Offshore Helideck Turbulent Flow," Vol. 29th International Conference on Ocean, Offshore and Arctic Engineering: Volume 6, June 2010, pp. 771–781.

[12] Rowe, S. J., Howson, D., and Turner, G., "A Turbulence Criterion for Safe Helicopter Operations to Offshore Installations," 30rd European Rotorcraft Forum, Marseille, France, 14-16th September 2004.

[13] Ewald, R., Peterka, J. A., and Cermak, J. E., "Wind-Tunnel Study of Wind over an OFFSHORE Platform Helideck," Tech. rep., Fluid Dynamics ad Diffusion Laboratory, Department of Civil Engineering, Colorado State University, December 1978, CER78-79RE-JAP-JEC25.

[14] Chen, Q., Gu, Z., Sun, T., and Song, S., "Wind environment over the helideck of an offshore platform," *Journal of Wind and Industrial Engineering*, Vol. 54-55, 1995, pp. 621–631.

[15] Rowe, S. J., Howson, D., and Turner, G., "A turbulence criterion for safe helicopter operations to offshore installations," *The Aeronautical Journal (1968)*, Vol. 110, No. 1113, 2006, pp. 749–758.

[16] Owen, I., White, M. D., Padfield, G. D., and Hodge, S. J., "A virtual engineering approach to the ship-helicopter dynamic interface – a decade of modelling and simulation research at the University of Liverpool," *The Aeronautical Journal*, Vol. 121, No. 1246, 2017, pp. 1833–1857.

[17] Oruc, I., Horn, J. F., Shipman, J., and Polsky, S., "Towards real-time pilot-in-the-loop CFD simulations of helicopter/ship dynamic interface," *International Journal of Modeling, Simulation, and*

Scientific Computing, Vol. 08, No. 04, 2017, pp. 1743005.

[18] Thedin, R., Kinzel, M. P., Horn, J. F., and Schmitz, S., "Coupled Simulations of Atmospheric Turbulence-Modified Ship Airwakes and Helicopter Flight Dynamics," *Journal of Aircraft*, Vol. 56, No. 2, 2019, pp. 812–824.

[19] Hodge, S. J., Forrest, J. S., Padfield, G. D., and Owen, I., "Simulating the environment at the helicopter-ship dynamic interface: research, development and application," *The Aeronautical Journal (1968)*, Vol. 116, No. 1185, 2012, pp. 1155–1184.

[20] Spalart, P. R., Deck, S., Shur, M. L., Squires, K. D., Strelets, M. K., and Travin, A., "New Version of Detached-eddy Simulation, Resistant to Ambiguous Grid Densities," *Theoretical and Computational Fluid Dynamics*, Vol. 20, No. 3, 2006, pp. 181–195.

[21] Forrest, J. S. and Owen, I., "An investigation of ship airwakes using Detached-Eddy Simulation," *Computers & Fluids*, Vol. 39, No. 4, April 2010, pp. 656–673.

[22] Watson, N. A., Kelly, M. F., Owen, I., Hodge, S. J., and White, M. D., "Computational and experimental modelling study of the unsteady airflow over the aircraft carrier HMS Queen Elizabeth," *Ocean Engineering*, Vol. 172, January 2019, pp. 562–574.

[23] Spalart, P. R., Jou, W. H., Strelets, M., and Allmaras, S. R., "Comments on the Feasibility of LES forWing and on a Hybrid RANS/LES Approach," 1st ASOSR Conference on DNS/LES, Ruston, Louisiana, August 1997, pp. 137–147.

[24] Garratt, R., *The Atmospheric Boundary Layer*, Cambridge Atmospheric and Space Science Series, Cambridge University Press, 1992.

[25] Hunt, J. C. R., Wray, A. A., and Moin, P., "Eddies, Streams, and Convergence Zones in Turbulent Flows," Tech. rep., Proceedings of the 1988 Summer Program, NASA Stanford Center for Turbulence Research, 1988, Report CTR-S88.

[26] White, M. D., Perfect, P., Padfield, G. D., Gubbels, A. W., and Berryman, A. C., "Acceptance Testing and Commissioning of a Flight Simulator for Rotorcraft Simulation Fidelity Research," *Proceedings of the Institution of Mechanical Engineers, Part G: Journal of Aerospace Engineering*, Vol. 227, No. 4, April 2013, pp. 663–686.

[27] Watson, N. A., Owen, I., and White, M. D., "Piloted Flight Simulation of Helicopter Recovery to the Queen Elizabeth Class Aircraft Carrier," *Journal of Aircraft*, Vol. 57, No. 4, 2020, pp. 742–760.

[28] Forrest, J. S., Owen, I., Padfield, G. D., and Hodge, S. J., "Ship-Helicopter Operating Limits Prediction Using Piloted Flight Simulation and Time-Accurate Airwakes," *Journal of Aircraft*, Vol. 49, No. 4, 2012, pp. 1020–1031.

[29] Forrest, J., Kaaria, C., and Owen, I., "Evaluating ship superstructure aerodynamics for maritime helicopter operations through CFD and flight simulation," *The Aeronautical Journal*, Vol. 120, No. 1232, 2016, pp. 1578–1603.

[30] Du Val, R. W. and He, C., "Validation of the FLIGHTLAB Virtual Engineering Toolset," *The Aeronautical Journal*, Vol. 122, No. 1250, April 2018, pp. 519–555.

[31] Howlett, J. J., "UH-60A Black Hawk Engineering Simulation Program: Volume I – Mathematical Model," Tech. rep., NASA, December 1981, NASA–CR–166309.

[32] Scott, P., White, M. D., and Owen, I., "The Effect of Ship Size on Airwake Aerodynamics and Maritime Helicopter Operations," 41rd European Rotorcraft Forum, Munich, Germany, 1 - 4th September 2015.

[33] "AC 29-2C Certification of Transport Category Rotorcraft," Tech. rep., United States Department of Transportation Federal Aviation Administration (FAA), July 2018.

[34] "C-29 Certification Specifications, Acceptable Means of Compliance and Guidance Material for Large Rotorcraft," Tech. rep., European Union Aviation Safety Agency (EASA), May 2022.

[35] Roscoe, A. and Ellis, G., "A Subjective Rating Scale for Assessing Pilot Workload in Flight: A Decade of Practical Use," Tech. rep., Royal Aerospace Establishment Farnborough, March 1990, RAE TR 90019.

[36] "Aeronautical Information Manual," Tech. rep., Federal Aviation Administration, May 2022.

[37] Carico, G. D., Fang, R., Finch, R. S., Geyer, Jr., W. P., Krijns, Cdr. (Ret.), H. W., and Long, K., "Helicopter/Ship Qualification Testing," Tech. rep., Research and Technology Organisation AGARDograph 300 Flight Test Techniques Series, February 2003, RTO AG-300 Vol. 22 / SCI-038.